Gibco-BRL). Double drug-resistant colonies were screened by Southern blotting with an LT–TNF-α intergenic probe. Homologous recombination was detected at a frequency of 1 in 63 drug-resistant colonies. Chimeric animals were obtained by injecting targeted cells into C57BL/6 blastocysts. Male mice showing >50% coat color chimerism were mated to C57BL/6 females, and germline transmission was documented by the presence of the 5.7-kb Pst I fragment.
22. I. Millet and N. H. Ruddle, *J. Immunol.*, in press.
23. Bioactivity of TNF-α–LT was measured with the WEHI 164 fibrosarcoma cell line as described [N. H. Ruddle *et al.*, *J. Exp. Med.* **172**, 1193 (1990)]. The specificity of the assay was defined with a neutralizing monoclonal antibody, TN3.19.12, that recognizes both murine TNF-α and LT.
24. Erythrocyte-depleted cells (10^6) were stained for 1 hour with fluoresceinated monoclonal antibodies to CD8 (Becton Dickinson), phycoerythrin-labeled monoclonal antibodies to CD4 (Becton Dickinson), fluoresceinated monoclonal antibodies to IgM (Pharmingen), phycoerythrin-labeled monoclonal antibodies to CD45R and B220 (Pharmingen), or biotinylated monoclonal antibodies to CD3ε (Pharmingen). The biotinylated monoclonal antibody was detected with streptavidin-RED613 (Gibco). Flow cytometric analysis was performed with the Lysis-I program (Becton Dickinson) on a FACScan (Becton Dickinson); data are means from experiments with three animals.
25. Cytolytic effector cells were established by primary, one-way mixed lymphocyte cultures of 1×10^7 to 2×10^7 $LT^{+/+}$ or $LT^{-/-}$ splenocytes ($H\text{-}2^b$) with 2×10^7 irradiated [absorbed dose of radiation (Gy) = 20 Gy] BALB/c ($H\text{-}2^d$) splenocytes. Responding cells were either unfractionated splenocytes, purified T cells (eluted from nylon wool then treated with monoclonal antibody J11d and complement), or purified $CD4^+$ T cells (eluted from nylon wool then treated with J11d and the CD8 monoclonal antibody 3.155 and complement). After culture for 5 to 6 days, live effector cells were isolated by Ficoll-Hypaque density gradient centrifugation. Target cells (0.5×10^6 to 1.0×10^6) were labeled in 1 ml of RPMI-1640 for 90 min with 500 μCi of $Na_2{}^{51}CrO_4$ or 10 μCi of 5′ ^{125}I-labeled iododeoxyuridine (^{125}I-UdR) as indicated, washed, incubated in the absence of label for 30 to 45 min, washed again, and added to varying numbers of effector cells. At the indicated times, release of label into the medium was assessed. After 6 hours, spontaneous ^{51}Cr release of P815 cells ($H\text{-}2^d$) was 7%, of TA3 cells ($H\text{-}2^d$) was 21%, and of EL-4 cells ($H\text{-}2^b$) was 5%. The nuclear lesion was assessed by termination of the incubation with 1 mM EDTA and 0.2% Triton X-100. Spontaneous release of ^{125}I-UdR was ≤14%.
26. J. H. Russell and C. B. Dobos, *J. Immunol.* **125**, 1256 (1980).
27. T. Ohsawa and S. Natori, *Dev. Biol.* **135**, 459 (1989).
28. E. Saksela and M. Jaatela, *Int. J. Dev. Biol.* **33**, 173 (1989).
29. M. L. Casey, S. M. Cox, B. Beutler, L. Milewich, P. C. MacDonald, *J. Clin. Invest.* **83**, 430 (1989).
30. M. S. Krangel, H. Yssel, C. Brocklehurst, H. Spits, *J. Exp. Med.* **172**, 847 (1990).
31. B. P. Giroir, T. Brown, B. Beutler, *Proc. Natl. Acad. Sci. U.S.A.* **89**, 4864 (1992).
32. S. de Kossodo *et al.*, *J. Exp. Med.* **176**, 1259 (1992).
33. K. Peppel, A. Poltorak, I. Melhado, F. Jirik, B. Beutler, *J. Immunol.* **151**, 5699 (1993).
34. K. Pfeffer *et al.*, *Cell* **73**, 457 (1993).
35. P. D. Crowe *et al.*, *Science* **264**, 707.
36. S. Miyawaki *et al.*, *Eur. J. Immunol.* **24**, 429 (1994).
37. We gratefully acknowledge P. M. Allen, L. E. Fields, M. Peters, and E. R. Unanue for helpful discussions concerning murine lymphoid development and lymph node and spleen architecture; O. Kanagawa for discussion of *aly* mice; C. Bergman for LT-TNF bioassays; B. Beutler at the University of Texas, Southwestern Medical School, for pMuCachectin cDNA; T. Doetschman at the University of Cincinnati for the D3 ES cell line; and E. R. Unanue for evaluation of murine histopathology. Supported in part by NIH grants CA 16885 (N.H.R.) and CA 28533 (J.H.R.), and National Multiple Sclerosis Society grant RG-2394 (N.H.R.). D.D.C. is an investigator of the Howard Hughes Medical Institute.

17 December 1993; accepted 11 March 1994

A Lymphotoxin-β–Specific Receptor

Paul D. Crowe, Todd L. VanArsdale, Barbara N. Walter, Carl F. Ware,* Catherine Hession, Barbara Ehrenfels, Jeffrey L. Browning, Wenie S. Din, Raymond G. Goodwin, Craig A. Smith

Tumor necrosis factor (TNF) and lymphotoxin-α (LT-α) are members of a family of secreted and cell surface cytokines that participate in the regulation of immune and inflammatory responses. The cell surface form of LT-α is assembled during biosynthesis as a heteromeric complex with lymphotoxin-β (LT-β), a type II transmembrane protein that is another member of the TNF ligand family. Secreted LT-α is a homotrimer that binds to distinct TNF receptors of 60 and 80 kilodaltons; however, these receptors do not recognize the major cell surface LT-α–LT-β complex. A receptor specific for human LT-β was identified, which suggests that cell surface LT may have functions that are distinct from those of secreted LT-α.

The TNF ligand family encompasses a large group of secreted and cell surface proteins that may affect the regulation of inflammatory and immune responses (*1*). Secreted forms of TNF and lymphotoxin-α (LT-α, previously referred to as TNF-β) are homotrimers (*2*) that initiate similar spectra of cellular responses by binding to two specific cell surface receptors of 60 and 80 kD ($TNFR_{60}$ and $TNFR_{80}$) (*3*). Membrane TNF, a type II transmembrane protein, is the precursor of secreted TNF (*4*); in contrast, cell surface LT is structurally different from secreted LT-α and TNF, which suggests that it may not bind to $TNFR_{60}$ or $TNFR_{80}$. Cell surface LT is a heteromeric complex composed of LT-α and LT-β subunits (*5*). Lymphotoxin-β is a type II transmembrane member of the TNF ligand family that provides the membrane anchor for the attachment of the heteromeric complex to the cell surface (*6*). To test if LT-β confers distinct receptor binding properties to the cell surface LT-α–LT-β complex, we used soluble versions of the TNFRs [engineered as fusion proteins between the ligand binding domain of TNFR and the Fc region of immunoglobulin G1 (IgG1) (TNFR:Fc)] as probes for membrane-bound cytokines (*7*).

Cell surface LT and TNF were rapidly induced on the human $CD4^+$ T cell hybridoma II-23 by phorbol myristate acetate (PMA), as detected by fluorescence staining with specific monoclonal antibodies (mAbs) (Fig. 1A) (*8*). Membrane TNF expression peaked 3 to 4 hours after stimulation with PMA and declined rapidly. In contrast, cell surface LT expression was maximal 6 to 8 hours after stimulation and remained detectable for more than 24 hours (Fig. 1B). The $TNFR_{60}$:Fc and $TNFR_{80}$:Fc chimeric proteins had similar staining patterns on II-23 cells activated for 6 hours with PMA (Fig. 1C). To determine which cell surface ligands bind $TNFR_{60}$:Fc, we used LT-α mAb (9B9) or TNF mAb (104C) competitively for staining of PMA-activated II-23 cells. Both of these mAbs block binding of the soluble ligands to TNFRs and directly neutralize cytotoxic function (*9*). In the presence of saturating concentrations of competitor mAb, specific staining for $TNFR_{60}$:Fc was partially blocked with an LT-α mAb (Fig. 1D) and more efficiently with a TNF mAb (Fig. 1E), which indicates that membrane TNF binds to $TNFR_{60}$. The latter finding is consistent with reports that membrane TNF is cytotoxic (*4*); however, these results also suggest that a less abundant form of the cell surface LT-α–LT-β complex may also be a ligand for $TNFR_{60}$ (Fig. 1D). In contrast, $TNFR_{60}$:Fc (or $TNFR_{80}$:Fc) did not bind to II-23 cells 24 hours after activation (Fig. 1F), despite the presence of substantial antigen detectable with LT-α mAb (compare to Fig. 1B).

These findings raised the possibility that a receptor other than $TNFR_{80}$ and $TNFR_{60}$ may recognize the major form of cell surface LT and prompted us to test other members of the TNFR family (*3*) for binding to cell

P. D. Crowe, T. L. VanArsdale, B. N. Walter, C. F. Ware, Division of Biomedical Sciences, University of California, Riverside, CA 92521, USA.
C. Hession, B. Ehrenfels, J. L. Browning, Biogen, Cambridge, MA 02142, USA.
W. S. Din, R. G. Goodwin, C. A. Smith, Immunex Research and Development, Seattle, WA 98101, USA.
*To whom correspondence should be addressed.

surface LT. We found that an Fc fusion construct of the TNF receptor–related protein (TNFRrp), a complementary DNA (cDNA) with sequence similarity to TNFR (*10*), bound II-23 cells when $TNFR_{60}$:Fc binding was low (Fig. 1F). Antibodies to TNF or LT-α did not block binding of TNFRrp:Fc to II-23 cells activated for 4 hours with PMA, and TNFRrp:Fc did not bind or neutralize cytotoxicity mediated by secreted LT-α or TNF (*11*), which provides additional evidence that TNF and LT-α are not ligands for TNFRrp.

The ligands recognized by TNFR:Fc and TNFRrp:Fc in biosynthetically labeled II-23 extracts were identified by receptor-mediated ligand precipitation (RMLP) with the use of the Fc fusion proteins in a manner analogous to that of antibodies in immunoprecipitation (*8, 12*). Both $TNFR_{60}$:Fc and LT-α mAb, but not TNFRrp:Fc, efficiently precipitated the LT-α (25 kD) that was secreted by II-23 cells (Fig. 2A). In the cell-associated fraction, which contains both LT-α homotrimers and LT-α–LT-β heteromeric complexes, $TNFR_{60}$:Fc coprecipitated LT-α (21 to 25 kD) and a small amount of LT-β (33 kD) (Fig. 2B). The band at 21 kD has previously been shown to be a precursor of mature LT-α (*5*). A second round of RMLP with $TNFR_{60}$:Fc failed to bind any additional ligand from this extract (Fig. 2B). In contrast, a third round of RMLP with TNFRrp:Fc bound an abundant amount of LT-α–LT-β complexes. In the reciprocal RMLP experiment, TNFRrp:Fc precleared a major fraction of the LT-α–LT-β complexes (Fig. 2B) but did not bind the complexes recognized by $TNFR_{60}$:Fc.

To unambiguously determine the specificity of TNFR:Fc and TNFRrp:Fc, we used recombinant baculovirus encoding either LT-α or a soluble form of LT-β to produce secreted LT-α–LT-β complexes by co-infection of BTI-TN-5B1-4 insect cells (*12, 13*). Soluble LT-β was created by deletion of the cytoplasmic and transmembrane regions and replacement with a type I leader sequence and a c-Myc decapeptide epitope (sLTβmyc) for detection with a mAb to Myc (*14*). RMLP analysis with either $TNFR_{60}$:Fc or TNFRrp:Fc of the ligands secreted by co-infected insect cells showed coprecipitation of LT-α and sLTβmyc proteins (Fig. 2C). In contrast, TNFRrp:Fc, but not $TNFR_{60}$:Fc, precipitated sLTβmyc from supernatants of cells infected with sLTβmyc virus alone (Fig. 2D), which indicates that TNFRrp:Fc is specific for LT-β. In light of the inability of TNFRrp to bind TNF or LT-α, we propose the more descriptive term LT-βR to denote this receptor.

LT-βR contains a cysteine-rich motif characteristic of the TNF–nerve growth factor family of transmembrane receptors homologous to $TNFR_{60}$ and $TNFR_{80}$. The

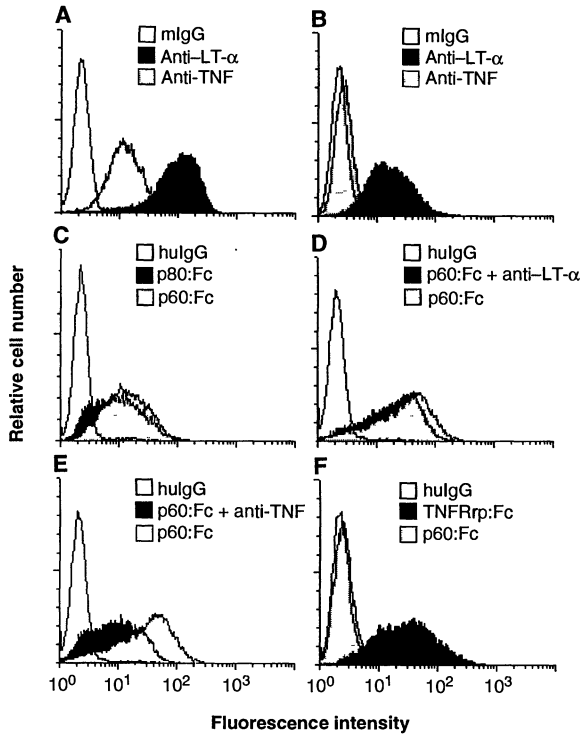

Fig. 1. Detection of TNF, LT-α, and LT-β on the surface of II-23 T cells by flow cytometry (*29*). Cells activated with PMA (25 ng/ml) for 4 hours (**A**) or 24 hours (**B**) were stained with mAbs to LT-α or TNF and PE-labeled goat antibody to mouse IgG (mIgG). (**C**) Cells activated with PMA for 6 hours were stained with $TNFR_{60}$:Fc (p60:Fc) or $TNFR_{80}$:Fc (p80:Fc) and goat antibody to human IgG-PE (huIgG). Cells treated with PMA for 6 hours were first incubated with mAbs to LT-α (**D**) or TNF (**E**) (25 μg/ml) as competitors, then stained with p60:Fc (2 μg/ml) and goat antibody to human IgG-PE. (**F**) II-23 cells activated with PMA for 24 hours were stained with p60:Fc or TNFRrp:Fc and goat antibody to human IgG-PE.

ligand binding domain of LT-βR is similar to that of $TNFR_{60}$ in the positional arrangement of cysteine residues in a CXXCXXC motif (where X is any amino acid) and the predicted size of the loops created by the disulfide bonds in domains 1 and 2; the latter is the major contact domain for LT-α (*15*). In contrast, domains 3 and 4 of LT-βR resemble those of $TNFR_{80}$ in the positioning of the cysteine residues and by the presence of a dramatically shortened loop 1 (5 versus 15 residues). An additional similarity between LT-βR and $TNFR_{80}$ is the membrane-proximal proline-rich region in the extracellular domain, which is thought to form a stalk extending the receptor from the cell surface. The cytoplasmic region of LT-βR has little sequence similarity with other members of the receptor family, which suggests that the mechanisms used to signal cellular responses may diverge from TNFR. The LT-βR has some similarity (over a short span) to the "death domain," which is present in Fas (*16*) and $TNFR_{60}$ (*17*); it is not yet known whether LT-β ligands mediate apoptosis or cytotoxicity. The gene that encodes LT-βR spans ~9 kb with an exon organization similar to that of $TNFR_{60}$ and is located on 12p13 as a cluster with CD27 and $TNFR_{60}$ (*18*).

Our data indicate that LT-α and LT-β combine to form soluble or membrane-anchored ligands that differ in receptor specificity. Secreted LT-α is a compact trimer with three identical receptor binding sites located in the surface cleft between neighboring subunits primarily in the a-a″ and d-e loops found on opposite sides of each subunit (*15, 19*). Structural similarity and molecular modeling indicate that LT-β may have a molecular architecture similar to that of LT-α, which suggests that a model for the surface LT complex should be a trimer in which subunits can assemble to form two complexes, $LT\alpha_1\beta_2$ and $LT\alpha_2\beta_1$. Cross-linking studies provided evidence for a stoichiometry of $LT\alpha_1\beta_2$ for the major cell surface LT complex (*5*). However, amino acids in LT-β corresponding to $TNFR_{60}$ contact residues of LT-α are not highly conserved, which predicts that a cleft formed between the LT-β and LT-α subunits in $LT\alpha_1\beta_2$ may not preserve the $TNFR_{60}$ binding site. The data presented here indicate that $TNFR_{60}$:Fc does not bind the major cell surface LT complex but rather binds a distinct complex with a predicted subunit ratio of $LT\alpha_2\beta_1$. In contrast, LT-βR:Fc binds to the major cell surface LT complex and to sLTβmyc but not to the ligands recognized by $TNFR_{60}$:Fc. The ligands that bind to LT-βR:Fc, $LT\alpha_1\beta_2$, and sLTβmyc are predicted to have a common cleft formed by neighboring LT-β subunits, analogous to the $TNFR_{60}$ binding site formed by adjacent LT-α subunits.

The multivalent ligands TNF and LT-α probably initiate cellular responses by inducing aggregation (clustering) of $TNFR_{60}$ or $TNFR_{80}$ (*20*). The model predicts that each LT-α–LT-β heterotrimer has a single receptor binding site composed of either an αα or ββ cleft and two distinct αβ clefts. Theoretically, these heteromeric ligands would be unable to induce clustering of either $TNFR_{60}$ or LT-βR and thus may function as

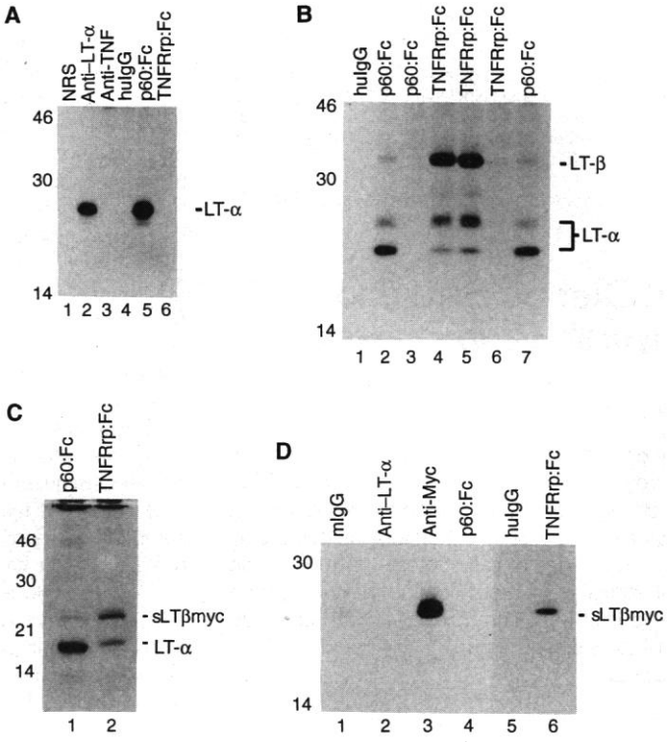

Fig. 2. Receptor-mediated ligand precipitation (RMLP) of LT-α–LT-β complexes. (**A**) Ligands secreted by II-23 cells. Culture supernatants from II-23 T cells were treated with PMA (25 ng/ml) for 4 hours and labeled with a mixture of [^{35}S]methionine and [^{35}S]cysteine for 15 min and subjected to immunoprecipitation with antibodies to either LT-α (lane 2) or TNF (lane 3) or RMLP with $TNFR_{60}$:Fc (p60:Fc) (lane 5) or TNFRrp:Fc (lane 6). Also shown are nonspecific precipitations with normal rabbit serum (NRS) (lane 1) or normal human IgG (huIgG) (lane 4). Precipitated proteins were resolved by reducing SDS–polyacrylamide gel electrophoresis (SDS-PAGE) (12% gel) and visualized by autoradiography. Molecular size standards (in kilodaltons) are shown at left. TNF was not visualized here because of its small amount. (**B**) Two populations of cell surface LT-α–LT-β complexes revealed by RMLP. II-23 cells activated and labeled as described above were extracted with detergent and subjected to RMLP by first preclearing twice with p60:Fc (lanes 2 and 3) and then precipitation with TNFRrp:Fc (lane 4); alternatively, the samples were reciprocally precleared with TNFRrp:Fc (lanes 5 and 6) and then by p60:Fc (lane 7). Nonspecific precipitation with normal human IgG is shown in lane 1. TNF was not visualized here because detergent dissociates the subunits (*30*), preventing binding to $TNFR_{60}$:Fc. (**C**) RMLP of soluble LT-α–sLTβmyc complexes. Culture supernatants (1 ml) from BTI-TN-5B1-4 cells co-infected with LT-α and sLTβmyc baculoviruses for 4 days (*12*) were subjected to RMLP with 5 μg of either p60:Fc (lane 1) or TNFRrp:Fc (lane 2). Proteins were analyzed by nonreducing SDS-PAGE (15% gel) and visualized by staining with Coomassie brilliant blue dye. (**D**) TNFRrp:Fc specificity for LT-β. Culture supernatants from BTI-TN-5B1-4 cells infected with sLTβmyc baculovirus and biosynthetically labeled with a mixture of [^{35}S]methionine and [^{35}S]cysteine (*12*) were subjected to immunoprecipitation with mAb to either LT-α (lane 2) or Myc (9E10) (lane 3) or to RMLP with either p60:Fc (lane 4) or TNFRrp:Fc (lane 6). Nonspecific precipitations with control murine IgG (lane 1) or normal human IgG (lane 5) are shown.

membrane-anchored antagonists of TNF or LT-α homotrimers or of a putative LT-β homotrimer. Alternatively, low-affinity binding to the αβ clefts by either TNFR or LT-βR may be sufficient to induce receptor aggregation. Another possibility that cannot be excluded is the existence of a receptor specific for the αβ clefts of $LT\alpha_2\beta_1$ or $LT\alpha_1\beta_2$, enabling these ligands to induce coclustering of distinct receptors including $TNFR_{60}$, $TNFR_{80}$, or LT-βR. The expression of cell surface LT-α–LT-β complexes by activated lymphocytes, such as cytotoxic T cells and interleukin-2 (IL-2)–stimulated natural killer cells (*21*), suggests the potential for these ligands to function as positive or negative regulators in inflammatory and immune responses. In this regard, members of the TNF ligand and receptor families appear to have important but divergent roles in immune regulation (*22, 23*). Targeted knockout of the murine LT-α gene disrupts peripheral lymphoid organ development (*24*). In contrast, genetic knockout of either $TNFR_{60}$ (*23*) or $TNFR_{80}$ (*25*) does not result in a similar phenotype, which suggests a role for the surface LT-α–LT-β complex and the LT-βR in immune development.

REFERENCES AND NOTES

1. C. A. Smith, T. Farrah, R. G. Goodwin, *Cell* **76**, 1959 (1994).
2. M. J. Eck and S. R. Sprang, *J. Biol. Chem.* **264**, 17595 (1989); M. Eck *et al.*, *ibid.* **267**, 2119 (1992); E. Y. Jones *et al.*, *Nature* **338**, 225 (1989).
3. C. A. Smith *et al.*, *Science* **248**, 1019 (1990); R. A. Heller *et al.*, *Proc. Natl. Acad. Sci. U.S.A.* **87**, 6151 (1990); H. Loetscher *et al.*, *Cell* **61**, 351 (1990); T. Schall *et al.*, *ibid.*, p. 361.
4. M. Kriegler *et al.*, *Cell* **53**, 45 (1988).
5. M. J. Androlewicz, J. L. Browning, C. F. Ware, *J. Biol. Chem.* **267**, 2542 (1992).
6. J. L. Browning *et al.*, *Cell* **72**, 847 (1993).
7. K. Peppel, D. Crawford, B. Beutler, *J. Exp. Med.* **174**, 1483 (1991). Receptor-Fc chimeric proteins were all constructed with a similar strategy, in which a cDNA encoding the extracellular domain of each receptor was joined to a cDNA encoding the hinge, CH2, and CH3 domains (amino acid residues 231 to 447) of human IgG1. Production of the $TNFR_{80}$:Fc and $TNFR_{60}$:Fc fusion proteins was as described (*12, 26*). Construction of a plasmid for expression of the TNFRrp:Fc fusion protein used polymerase chain reaction (PCR) amplification to obtain the extracellular domain of TNFRrp. The 5′ oligonucleotide used in this reaction was 5′-ATAGCGGCCGC-CATGCTCCTGCC- TT-3′, which introduces a Not I site upstream of the initiator methionine. The 3′ antisense oligonucleotide used was 5′-ATAAGATC-TGGGCTCCATCAGCATGGTTCCTGACATCTC-3′, which is preceded by a Bgl II cleavage site that allows for its subsequent ligation to the Fc domain of a human IgG1 sequence (*27*). The PCR reaction was done with a cDNA template synthesized from RNA derived from human peripheral blood lymphocytes that had been stimulated with phytohemagglutinin for 24 hours. Expression and purification of the TNFRrp:Fc fusion protein was as described (*27*).
8. J. L. Browning, M. J. Androlewicz, C. F. Ware, *J. Immunol.* **147**, 1230 (1991).
9. C. M. Liang *et al.*, *Biochem. Biophys. Res. Commun.* **137**, 847 (1986); C. F. Ware and P. D. Crowe, unpublished data.
10. M. Baens *et al.*, *Genomics* **16**, 214 (1993).
11. C. F. Ware, P. D. Crowe, C. A. Smith, unpublished observations.
12. P. D. Crowe *et al.*, *J. Immunol. Methods* **168**, 79 (1994).
13. Soluble LTβmyc was constructed with a type I signal sequence cassette from a Hind III restriction digest of vascular cell adhesion molecule–1 (VCAM-1) in pCDM8 (*28*), and subsequent repair of the 5′ overhang was done with the Klenow fragment of DNA polymerase I, which was digested with Not I and gel-purified to obtain the fragment from nucleotides 1 to 178. The c-Myc fragment, a 51-bp oligonucleotide (5′-GAACAGAAACTCATCTCTGAAGAAGA-CCTGGGGTTTCAGAAGCTGCCAGAG-3′), and its complement were synthesized, annealed, and digested with Alw NI. The LT-β–pCDM8 cDNA (*6*) was digested with Alw NI and Not I, and a 675-bp fragment corresponding to nucleotides 228 to 898 was gel purified. The three fragments were ligated into pCDM8 that had a modified polylinker. For insect cell expression, a Hind III 910-bp fragment from LTβmyc-pCDM8 was purified and ligated into Hind III–digested BlueBacIII (Invitrogen), and recombinant virus was obtained by transfection of BTI-TN-5B1-4 insect cells. Production of LT-α baculovirus was as described (*12*).
14. S. Munro and H. R. Pelham, *Cell* **46**, 291 (1986).
15. D. W. Banner *et al.*, *ibid.* **73**, 431 (1993).
16. N. Itoh and S. Nagata, *J. Biol. Chem.* **268**, 10932 (1993).
17. L. A. Tartaglia *et al.*, *Cell* **74**, 845 (1993).
18. P. Marynen, personal communication.
19. C. Goh and A. Porter, *Protein Eng.* **4**, 385 (1991); X. Van Ostade, J. Tavernier, T. Prangé, W. Fiers, *EMBO J.* **10**, 827 (1991).
20. H. Engelmann *et al.*, *J. Biol. Chem.* **265**, 14497 (1990); D. Pennica *et al.*, *Biochemistry* **31**, 1134 (1992); D. Pennica *et al.*, *ibid.* **32**, 3131 (1993).
21. C. F. Ware *et al.*, *J. Immunol.* **149**, 3881 (1992).
22. R. C. Allen *et al.*, *Science* **259**, 990 (1993); R. Watanabe-Fukunaga *et al.*, *Nature* **356**, 314 (1992); U. Korthäuer *et al.*, *ibid.* **361**, 539 (1993); J. P. DiSanto *et al.*, *ibid.*, p. 541; G. Messer *et al.*, *J. Exp. Med.* **173**, 209 (1991).
23. J. Rothe *et al.*, *Nature* **364**, 798 (1993); K. Pfeffer *et al.*, *Cell* **73**, 457 (1993).
24. P. De Togni *et al.*, *Science* **264**, 703 (1994).
25. M. Moore, personal communication.
26. K. M. Mohler *et al.*, *J. Immunol.* **151**, 1548 (1993).
27. W. C. Fanslow *et al.*, *ibid.* **149**, 655 (1992).
28. L. Osborn *et al.*, *Cell* **59**, 1203 (1989).
29. Cells washed in RPMI-1640 containing 10% fetal bovine serum, 0.1% sodium azide, and 20 mM Hepes (pH 7.2) (binding buffer) were resuspended in the same buffer supplemented with human IgG (50 μg/ml) and incubated with TNFR:Fc constructs (5 μg/ml), mAb to TNF or LT (5 μg/ml), or rabbit LT polyclonal antisera (1:250 dilution) for

30 to 60 min on ice. The cells were washed twice with binding buffer then incubated with a 1:500 dilution of phycoerythrin (PE)-labeled goat antibody to human IgG, goat antibody to mouse IgG, or goat antibody to rabbit IgG (Calbiochem, San Diego, CA) for 30 min. Similar concentrations of isotype-matched control antibodies or normal rabbit serum were used to determine nonspecific staining. Analyses were done with a FACScan instrument and LYSIS II software (Becton Dickinson, Mountain View, CA).

30. J. L. Browning and A. Ribolini, *J. Immunol.* **143**, 1859 (1989).

31. Supported in part by grants (to C.F.W.) from the American Cancer Society (IM663) and the Tobacco Surtax Fund of the State of California through the Tobacco-Related Diseases Research Program (RT0261).

11 January 1994; accepted 14 March 1994

Effects of Manipulated Diet on Size and Performance of Brachyuran Crab Claws

L. David Smith*† and A. Richard Palmer

Crabs grown experimentally on fully shelled prey developed larger and stronger claws than those raised on nutritionally equivalent unshelled prey. When one claw was immobilized, claws also became asymmetrical. These use-induced changes differ from skeletal remodelling in vertebrates and many invertebrates because changes in the rigid exoskeleton can occur only after molting, and claw muscle mass must be reduced substantially before the molt. Such short-term adaptive responses to environmental stimuli, if heritable, could yield long-term evolutionary changes in claw size and, if combined with behavioral biases toward one side (handedness), could also promote the evolution of claw dimorphism.

The form of biological structures can be developmentally sensitive or insensitive to environmental conditions. Plasticity, however, may be either adaptive or nonadaptive depending on whether fitness is altered in individuals whose form has changed (*1, 2*). In addition, plasticity may either accelerate the rate of evolution by generating phenotypic variation or retard it by reducing the concordance between genotypes and phenotypes (*3–5*). Phenotypic plasticity can thus be significant on both ecological and evolutionary time scales. Although numerous predators induce changes that make prey more resistant (*6–8*), relatively little is known about how sensitive predator form is to differences in prey toughness, because previous studies have had difficulty separating nutritional effects from use-induced effects in fishes (*9–11*) and insects (*12*). Adaptive plasticity in predator feeding structures may have contributed to the coevolutionary arms race between durophagous predators and shelled prey (*13*).

We tested the effect of diet toughness on both claw form and performance of the brachyuran crab, *Cancer productus*. Brachyuran crabs include many ecologically important predators that use their claws to subjugate shelled prey (*14*). Claw size and leverage properties determine crushing force (*15, 16*), and induction or reversal of claw asymmetry after autotomy in certain heterochelous species suggests substantial developmental lability (*17–19*). But because of constraints imposed on muscle volume by a rigid exoskeleton and because of extensive muscle atrophy before molting, we don't know whether differential use can affect subsequent form in crustaceans.

Cancer productus is a common molluscivorous crab in estuaries and bays of the northeastern Pacific Ocean (*20*). Field-collected juveniles were held in running-seawater aquaria at the Bamfield Marine Station, Bamfield, British Columbia (*21*). Roughly equal numbers of male and female crabs were assigned randomly to one of four treatments that manipulated use of the claws (Table 1). Before the first molt in captivity, all crabs had full use of both claws and were fed an excess of small, intact mussels (*Mytilus*) well below the maximum size they could crush. After the first molt, by which time crabs were nearing maturity, all crabs were placed on their respective experimental diets. Crabs on a hard diet (H) received intact, closed mussels within 20% of the maximum size they could crush (*22*). Those on a soft diet (S) received similarly sized, opened mussels, where the flesh was easily accessible. For half of the individuals on each diet type, either a right or left claw was glued closed at random with cyanoacrylate glue within 48 hours after the first and all subsequent molts in captivity. By using only *Mytilus* as food, we avoided potentially confounding nutritional differences among treatments that have complicated interpretation of diet-induced effects elsewhere (*9, 11, 12*). Crabs were reared through one or two entire intermolt cycles on the experimental diets, and crushing forces were measured after the second molt (*23*). Claw measurements were obtained from preserved exoskeletons (*24*).

We examined the effects of diet toughness on relative claw size by computing the approximate volume of the manus (the portion of the claw excluding the fingers) (*24*) for each molt of each crab and adjusting for differences in overall crab size (*25*). For one analysis, we also computed a standardized claw size by adjusting for differences in relative claw size among individuals in the pretreatment molt. Differences in relative claw size among the six treatments (note that glued and free claws in the one-claw glued treatments were analyzed separately) were tested with

Table 1. Sample sizes, carapace widths, and intermolt durations of *C. productus* used in the experiments. (See legend to Fig. 1 for a description of "Origin of molt" categories and experimental group labels.) nr, not relevant.

	Origin of molt			
	Field	Pre-treatment	Expt. 1	Expt. 2
	*Number of crabs in each treatment**			
Hard diet, both claws free (H2)	12	12	8	8
Soft diet, both claws free (S2)	13	13	11	5
Hard diet, one claw glued (H1)	13	13	10	8
Soft diet, one claw glued (S1)	13	13	12	7
Total	51	51	41	28
	Carapace width (mm)†			
Mean	32.8	44.0	57.3	68.6
Standard error	0.80	1.10	1.65	2.18
	Intermolt duration (days)			
Mean	nr	31.7	52.0	75.9
Standard error		1.91	2.12	5.97

*For treatments H1 and S1, the number of claws per analysis was equal to the number of crabs, but for H2 and S2, it was twice the number of crabs. †Carapace widths did not differ between sexes nor among treatments at any of the four molts ($P > 0.2$, two-way ANOVA, Sex X Treatment for each molt).

Department of Zoology, University of Alberta, Edmonton, Alberta, T6G 2E9, and Bamfield Marine Station, Bamfield, British Columbia V0R 1B0, Canada.

*Present address: Smithsonian Environmental Research Center, Post Office Box 28, Edgewater, MD 21037, USA.

†To whom correspondence should be addressed.